


## Noise intensity of a Markov chain

Lukas Ramlow  and Benjamin Lindner <sup>\*</sup>

*Bernstein Center for Computational Neuroscience Berlin, Philippstrasse 13, Haus 2, 10115 Berlin, Germany  
and Physics Department of Humboldt University Berlin, Newtonstrasse 15, 12489 Berlin, Germany*

 (Received 16 February 2024; accepted 8 July 2024; published 25 July 2024)

Stochastic transitions between discrete microscopic states play an important role in many physical and biological systems. Often these transitions lead to fluctuations on a macroscopic scale. A classic example from neuroscience is the stochastic opening and closing of ion channels and the resulting fluctuations in membrane current. When the microscopic transitions are fast, the macroscopic fluctuations are nearly uncorrelated and can be fully characterized by their mean and noise intensity. We show how, for an arbitrary Markov chain, the noise intensity can be determined from an algebraic equation, based on the transition rate matrix; these results are in agreement with earlier results from the theory of zero-frequency noise in quantum mechanical and classical systems. We demonstrate the validity of the theory using an analytically tractable two-state Markovian dichotomous noise, an eight-state model for a calcium channel subunit (De Young-Keizer model), and Markov models of the voltage-gated sodium and potassium channels as they appear in a stochastic version of the Hodgkin-Huxley model.

DOI: [10.1103/PhysRevE.110.014139](https://doi.org/10.1103/PhysRevE.110.014139)

### I. INTRODUCTION

For models of many fluctuation phenomena in physics, biology, chemistry, and other fields, it is important to properly characterize the noise that drives a given dynamical system. Examples include the firing of a neuron, driven by channel noise [1–6] and by shot-noise-like input from other neurons [7–12], the fluctuations in the intensity of an excitable laser [13–16], or chemical reactions in mesoscopically small volumes [17–19]. In the past decades, strongly simplified noise models, such as white Gaussian noise, Poissonian shot noise, dichotomous noise, or an exponentially correlated Ornstein-Uhlenbeck noise have often been used to describe the input noise in these systems. As the models for the driving noise process become more complex, one would like to use characteristics of the noise process that can be used to fairly compare different noise models (and their effect on a dynamical system). This fair comparison is already possible for simple noise processes, such as different exponentially correlated processes like the Gaussian Ornstein-Uhlenbeck process [20–22], the dichotomous telegraph noise [17,23–25], or the exponentially distributed noise [26] (which is, however, only approximately exponentially correlated).

Simple characteristics of a stochastic (noise) process  $x(t)$  are its stationary mean and variance

$$\mu = \langle x(t) \rangle, \quad \sigma^2 = \langle \Delta x^2 \rangle = \langle x^2(t) \rangle - \langle x(t) \rangle^2, \quad (1)$$

its correlation time

$$\tau = \int_0^\infty dt' \frac{\langle x(t)x(t+t') \rangle - \langle x(t) \rangle^2}{\langle \Delta x^2 \rangle}, \quad (2)$$

and its noise intensity

$$D = \int_0^\infty dt' \langle x(t)x(t+t') \rangle - \langle x(t) \rangle^2. \quad (3)$$

The meaning of mean and variance are quite obvious. The correlation time (here defined by an integral over the normalized autocorrelation function) provide an order-of-magnitude estimate of the periods over which the process changes significantly. Last but not least, the intensity (here defined by an integral over the *unnormalized* autocorrelation function) captures how much of an effect the process would have when driving a dynamical system. More specifically, if  $x(t)$  were the velocity of a Brownian particle,  $D$  would correspond to the diffusion coefficient, which is a reasonable measure of the effect of the velocity noise on the position dynamics. An alternative interpretation is based on the observation that the integral is a (half of a symmetric) Fourier transform of the correlation function at zero frequency, i.e.,  $D$  can be regarded as the zero-frequency limit of the fluctuation's power spectrum.

It is clear from the above definitions that correlation time, variance, and intensity are connected by

$$D = \sigma^2 \tau, \quad (4)$$

i.e., if we know two of the characteristics, we can easily compute the third one. For processes described by a nonlinear Langevin equation, all four characteristics (including also the mean value) can be expressed by quadratures [27]; see also Refs. [28,29], which include making the above-mentioned connection between noise intensity and diffusion coefficient more explicit.

For discrete-valued processes,  $x(t) \in \{x_1, x_2, \dots\}$ , governed by a master equation, the mean and the variance can easily be calculated in all cases where the stationary probability can be obtained. The calculation of the noise intensity is more involved but has recently been worked out in our previous paper and applied for a specific model [30,31]. In fact, the general solution to the problem has been given in the community dealing with zero-frequency current noise decades ago [32,33] and generalized to quantum mechanical systems

<sup>\*</sup>Contact author: [benjamin.lindner@physik.hu-berlin.de](mailto:benjamin.lindner@physik.hu-berlin.de)

[34]. Here, we rederive the theory for a general master equation in a hopefully accessible way and apply the resulting formulas to popular models of channel kinetics.

Our paper is structured as follows. We begin in Sec. II with the general framework for calculating the noise intensity. Then we discuss three examples. In Sec. III we illustrate the general result for the (simple and well-known) case of Markovian dichotomous noise. In Sec. IV we study the more complicated case of an eight-state Markov model, as used in the De Young-Keizer model to describe a subunit of calcium release channel. In Sec. V we study a stochastic version of the sodium and potassium currents as they appear in the Hodgkin-Huxley model with channel noise. Finally, in Sec. VI, we discuss further applications of our results, such as a general white-noise approximation in cases where the microscopic transitions are much faster than the dynamics of the driven system. However, we also point out some limitations for systems where the noise is *not* purely external and/or very fast but also depends on the state of the driven system.

## II. NOISE INTENSITY OF A MARKOV CHAIN

We consider a random process  $x(t)$  with discrete states, where the probability  $p_i(t)$  of finding a state  $i$  at time  $t$  is determined by the (homogeneous) master equation

$$\dot{\mathbf{p}}(t) = W\mathbf{p}(t), \quad (5)$$

with the probability vector  $\mathbf{p}(t) = (p_1(t) \ p_2(t) \ \dots)$  and the transition rate matrix  $W = (w_{ij})$ . The entries  $w_{ij} > 0$  for  $i \neq j$  are the transition rates from a state  $j$  to state  $i$  and  $w_{jj} = -\sum_{i \neq j} w_{ij}$ . To fully characterize the process  $x(t)$ , each state  $i$  is assigned a specific value  $x_i$ , which are not necessarily different from each other.

For such a random process, the calculation of the mean and the variance follows standard procedures [17,18] and is based on the stationary probability vector  $\lim_{t \rightarrow \infty} \mathbf{p}(t) = \mathbf{p}$  (we indicate the stationary state by omitting the time argument). This vector can be obtained from the stationary master equation

$$0 = W\mathbf{p}, \quad (6)$$

together with the normalization condition  $\sum_i p_i = 1$ ; the additional condition is needed because of the rank deficiency of the matrix  $W$ . Practically, the normalization can be incorporated by replacing an arbitrary row of the matrix  $W$  with ones and the corresponding entry in the zero vector on the left-hand side (l.h.s.) by a one. This leads to a linear system of equations solvable by standard methods. Given the stationary probabilities  $p_i$ , the mean and the variance can be calculated by

$$\mu = \sum_i x_i p_i, \quad \sigma^2 = \sum_i (x_i - \mu)^2 p_i. \quad (7)$$

The calculation of the noise intensity is more advanced. We recall the definition of the noise intensity by the integral over the autocorrelation function Eq. (3). In principle, the correlation function can be determined by solving the time-dependent master Eq. (5). However, it turns out that the calculation of the time-dependent probability vector  $\mathbf{p}(t)$  is not necessary to calculate the noise intensity. Instead, taking advantage of the fact that the integrated correlation function is

of interest, an algebraic equation can be found that determines the noise intensity and is not much more complicated to solve than the equations that determine the mean or variance. We emphasize that this approach has been put forward much earlier in different contexts [30,32–34].

To show this, we relate the noise intensity to the probabilities of the Markov chain

$$\begin{aligned} D &= \int_0^\infty dt' \langle x(t+t')x(t) \rangle - \langle x(t) \rangle^2 \\ &= \int_0^\infty dt' \sum_{i,j} [x_i x_j p_{ij}(t') p_j - x_i x_j p_i p_j] \\ &= \sum_{i,j} x_i f_{ij} x_j p_j, \end{aligned} \quad (8)$$

where  $p_{ij}(t') = p(i, t+t'|j, t)$  is the transition probability, i.e., the probability of finding the state  $i$  at  $t+t'$  given the state  $j$  at time  $t$ . Since we are considering a homogeneous process, this conditional probability does not depend on the absolute time  $t$ , but only on the difference  $t'$  and is determined by the master Eq. (5) with the initial condition  $p_k(t) = \delta_{kj}$ . The auxiliary function introduced in the last line of Eq. (8),

$$f_{ij} = \int_0^\infty dt' p_{ij}(t') - p_i, \quad (9)$$

is given by the integral over the difference between the transition and stationary probabilities. Equation (8) is of course just a reformulation of the problem. However, it turns out that the auxiliary functions  $f_{ij}$  for a given  $j$  can be calculated from a system of algebraic equations together with an additional condition, a calculation that is very similar to that of the stationary probabilities  $p_i$ . To see this, we formulate the master equation where the state at some reference time  $t$  has been specified [ $p_{kj}(0) = \delta_{kj}$ ]:

$$\begin{aligned} \dot{p}_{kj}(t') &= \sum_i w_{ki} p_{ij}(t'), \\ \dot{p}_{kj}(t') &= \sum_i w_{ki} [p_{ij}(t') - p_i], \\ p_k - \delta_{kj} &= \sum_i w_{ki} f_{ij}. \end{aligned} \quad (10)$$

To get from the first to the second line we subtracted the stationary master equation  $0 = \sum_i w_{ki} p_i$ . To get from the second to the third line we integrated over  $t'$ , used Eq. (9), and exploited that  $\int_0^\infty dt' \dot{p}_{kj}(t') = p_k - \delta_{kj}$ . The last line in Eq. (10) looks like an equation that uniquely determines  $f_{ij}$ . However, because of the rank deficiency of  $W$  we need an additional condition that is obtained by observing that

$$\sum_i f_{ij} = \int_0^\infty dt' \sum_i [p_{ij}(t') - p_i] = 0. \quad (11)$$

This condition is independent of  $j$  and reflects that for any  $t'$  both the transition probability and the stationary probability are normalized over the states  $i$ .

Finally, while Eqs. (8) to (11) allow for the calculation of noise intensity, they can be expressed more conveniently. For

this purpose, we write Eq. (8) in matrix notation

$$D = \mathbf{x}^T F \mathbf{y}, \quad (12)$$

where  $f_{ij}$  is the entry in the  $i$ th row and  $j$ th column of the matrix  $F$  and the two vectors are given by  $\mathbf{x} = (x_1 \ x_2 \ \dots)^T$  and  $\mathbf{y} = (x_1 p_1 \ x_2 p_2 \ \dots)^T$ . Similarly, the set of linear Eqs. (10) can be combined into a single matrix equation

$$P - \mathbb{1} = W F, \quad (13)$$

where  $P$  is a matrix in which each entry in the  $i$ th row is given by the stationary probability  $p_i$  and  $\mathbb{1}$  is the identity matrix. The additional condition Eq. (11) can be written as

$$(1 \ 1 \ \dots \ 1)F = 0, \quad (14)$$

implying that each column of the matrix  $F$  adds up to zero. Again, practically, these conditions can be incorporated by replacing an arbitrary row in  $W$  by ones and the corresponding row of the matrix  $P - \mathbb{1}$  by zeros. The analytical expressions Eq. (6) for the stationary probability vector  $\mathbf{p}$  and Eq. (13) for the auxiliary matrix  $F$  are equivalent to Eqs. (43) and (44) in Ref. [34], which are needed to compute the zero-frequency power spectrum, i.e., the noise intensity.

In the following, we put the theory to the test for different models. The first model is the well-known Markovian two-state model, the second is a more involved eight-state model for a subunit of a calcium channel (De Young-Keizer model), and the third example comprises the Sodium and potassium channels in a stochastic version of the Hodgkin-Huxley model of an excitable nerve membrane.

To compute the statistics of interest in stochastic simulations, we follow standard procedures to obtain the time series  $x(t)$  [35]. We choose an initial state  $j$  at time  $t_0 = 0$  and simulate the stochastic sequence of states at (discrete) times  $t_1 < t_2 < \dots < t_N$  with fixed step size  $\Delta t = t_{i+1} - t_i$  (for specific values, see figure captions). At each time, the stimulation is performed in two steps. In a first step, we determine whether the state of the Markov chain changes over the interval  $\Delta t$ . To this end, we calculate the transition probability  $P_j = \sum_{i \neq j} w_{ij} \Delta t$  (recall that  $w_{ij}$  denotes the transition rate from a state  $j$  to a state  $i$ ) and compare it to a random number  $\eta_1$  that is uniformly distributed over the interval  $[0, 1]$ ; the step size  $\Delta t$  must be chosen so that  $P_j \ll 1$ . If  $\eta_1 < P_j$ , the state of the model changes and, in a second step, the specific state attained is determined. To this end, we draw a second random number  $\eta_2$ , uniformly distributed over the interval  $[0, \sum_{i \neq j} w_{ij}]$ . If this number falls in the interval  $[\sum_{i < k} w_{ij}, \sum_{i < k+1} w_{ij}]$ , the model attains the state  $k$  which is associated with  $x(t) = x_k$ .

Finally, we numerically determine the mean, variance, and noise intensity from the time series  $x(t)$ . Both mean and variance are computed as time averages  $\mu = \int_0^{t_N} dt x(t)/t_N$  and  $\sigma^2 = \int_0^{t_N} dt [x(t) - \mu]^2/t_N$ , respectively; the expression become exact for  $N \rightarrow \infty$ , here we take a sufficiently large value  $N = 10^7$ . To compute the noise intensity, we introduce the smoothed process  $X(t; T) = \int_t^{t+T} dt x(t)/T$  and use that its variance  $\sigma_X^2(T)$  is related to the noise intensity by  $D = \lim_{T \rightarrow \infty} \sigma_X^2(T)T/2$ ; in practice  $T$  must be chosen much larger than the correlation time of the process  $x(t)$  which depends on the specific model (for specific values, see figure captions).

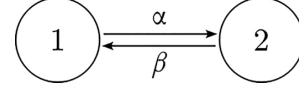


FIG. 1. State diagram of a dichotomous noise. The system consists of two states 1 and 2 with corresponding levels  $x_1$  and  $x_2$ . The transitions between the two states occur at rates  $\alpha$  and  $\beta$ .

### III. A SIMPLE EXAMPLE: MARKOVIAN DICHOTOMOUS NOISE

As an introduction to the method, we consider a Markovian dichotomous noise for which the noise intensity is known and can be calculated in several ways [23]. A dichotomous Markov noise  $x(t)$  is a Markov process with two levels  $x_1$  and  $x_2$ , corresponding to two different states with transition rates  $\alpha$  and  $\beta$  between them. A schematic representation of the model is shown in Fig. 1.

To calculate the noise intensity according to Eq. (12), we first determine the stationary probabilities using the stationary master Eq. (6)

$$0 = \begin{pmatrix} -\alpha & \beta \\ \alpha & -\beta \end{pmatrix} \begin{pmatrix} p_1 \\ p_2 \end{pmatrix}, \quad (15)$$

together with the normalization condition  $p_1 + p_2 = 1$  and obtain  $p_1 = \beta/(\alpha + \beta)$  and  $p_2 = \alpha/(\alpha + \beta)$ . We can now calculate  $F$  using Eq. (13)

$$\begin{pmatrix} p_1 & p_1 \\ p_2 & p_2 \end{pmatrix} - \begin{pmatrix} 1 & 0 \\ 0 & 1 \end{pmatrix} = \begin{pmatrix} -\alpha & \beta \\ \alpha & -\beta \end{pmatrix} \begin{pmatrix} f_{11} & f_{12} \\ f_{21} & f_{22} \end{pmatrix} \quad (16)$$

with the additional conditions that each column of  $F$  sums to zero, i.e.,  $f_{11} + f_{21} = 0$  and  $f_{12} + f_{22} = 0$ . This yields

$$F = \frac{1}{(\alpha + \beta)^2} \begin{pmatrix} \alpha & -\beta \\ -\alpha & \beta \end{pmatrix} \quad (17)$$

and allows to determine the noise intensity using Eq. (12)

$$\begin{aligned} D &= \frac{1}{(\alpha + \beta)^3} (x_1 \ x_2) \begin{pmatrix} \alpha & -\beta \\ -\alpha & \beta \end{pmatrix} \begin{pmatrix} x_1 \beta \\ x_2 \alpha \end{pmatrix} \\ &= \frac{\alpha \beta}{(\alpha + \beta)^3} (x_1 - x_2)^2, \end{aligned} \quad (18)$$

an expression that is in agreement with the result presented in Ref. [23]. The noise intensity has a maximum as a function of the rate  $\alpha$ , keeping the other rate  $\beta$  fixed, at  $\alpha^* = \beta/2$  [Fig. 2(a)]. As a function of the correlation time  $\tau = 1/(\alpha + \beta)$  has also a maximum at  $\tau^* = 2/(3\beta)$  [Fig. 2(b)]. If the intensity is plotted as a function of the ratio  $x_1/x_2$  (Fig. 2(c)), it has a minimum and vanishes for  $x_1^* = x_2$  because the variance vanishes in this case. When plotted as a function of the variance  $\sigma^2$  [Fig. 2(d)], the noise intensity increases linearly according to Eq. (4).

The calculation presented here serves only as a sanity check. The real advantage of the method lies in the possibility of calculating the noise intensity for more complicated transition rate matrices, as we will show in the following.

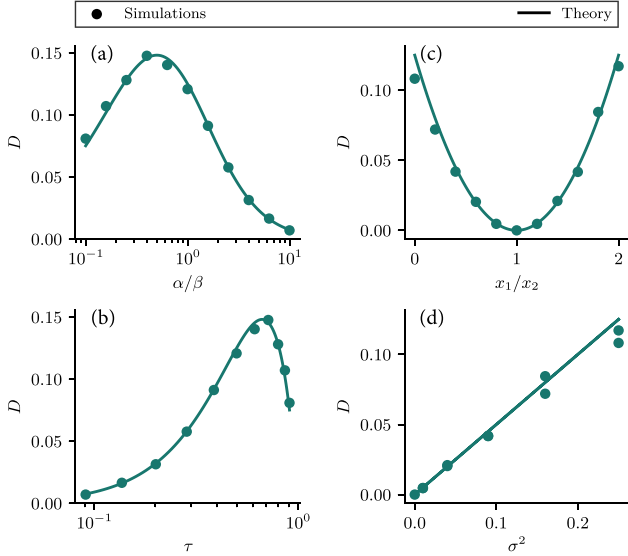


FIG. 2. The noise intensity of a Markovian Dichotomous noise. Panels (a), (b) show the noise intensity as a function of the ratio between the transition rates  $\alpha/\beta$  or the correlation time  $\tau = 1/(\alpha + \beta)$ . The intensity has a maximum at  $\alpha^* = \beta/2$  or  $\tau^* = 2/(3\beta)$ . Panels (c), (d) show the noise intensity as a function of the values taken in the two states  $x_1/x_2$  or the variance  $\sigma^2 = \alpha\beta(x_1 - x_2)^2/(\alpha + \beta)^2$ . The intensity has a minimum at  $x_1^* = x_2$  and scales linearly with the variance. Parameters:  $\beta = 1$ ,  $x_2 = 1$  and  $\Delta t = 10^{-2}$ ,  $T = 200$ .

#### IV. A BIOPHYSICAL EXAMPLE: STOCHASTIC $\text{Ca}^{2+}$ CHANNEL MODEL

In this section, we consider a biophysical example and calculate the noise intensity for a eight-state Markov model as illustrated in Fig. 3 and used in the De Young-Keizer model to describe a single subunit of an inositol trisphosphate ( $\text{IP}_3$ ) receptor [36]. For such a model, no closed-form expression for the noise intensity is known.

The entire De Young-Keizer model describes the dynamics of the intracellular calcium ( $\text{Ca}^{2+}$ ) concentration, which in many cells serves as a signaling molecule to transmit infor-

TABLE I. Simulation parameters for a  $\text{IP}_3$ -receptor subunit in the De Young-Keizer model [36].

Parameter	Value	Description
binding constants		
$\hat{\alpha}_1 (\mu\text{M}^{-1}\text{s}^{-1})$	400	$\text{IP}_3$
$\hat{\alpha}_2 (\mu\text{M}^{-1}\text{s}^{-1})$	0.2	$\text{Ca}^{2+}$ inhibition
$\hat{\alpha}_3 (\mu\text{M}^{-1}\text{s}^{-1})$	400	$\text{IP}_3$
$\hat{\alpha}_4 (\mu\text{M}^{-1}\text{s}^{-1})$	0.2	$\text{Ca}^{2+}$ inhibition
$\hat{\alpha}_5 (\mu\text{M}^{-1}\text{s}^{-1})$	20	$\text{Ca}^{2+}$ activation
dissociation constants $\gamma_i = \beta_i/\hat{\alpha}_i$		
$\gamma_1 (\mu\text{M})$	0.13	$\text{IP}_3$
$\gamma_2 (\mu\text{M})$	1.049	$\text{Ca}^{2+}$ inhibition
$\gamma_3 (\text{nM})$	943.4	$\text{IP}_3$
$\gamma_4 (\text{nM})$	144.5	$\text{Ca}^{2+}$ inhibition
$\gamma_5 (\text{nM})$	82.34	$\text{Ca}^{2+}$ activation

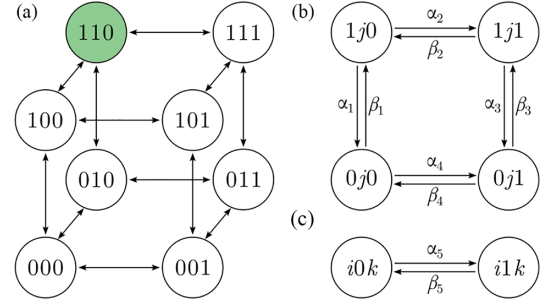


FIG. 3. State diagram of a  $\text{Ca}^{2+}$  channel subunit [36]. Panel (a) shows the eight-state model of a single  $\text{IP}_3$ -receptor subunit. The states are denoted  $ijk$ , where each index represents one of the three binding sites for  $\text{IP}_3$  ( $i$ ), activating  $\text{Ca}^{2+}$  ( $j$ ), and inhibitory  $\text{Ca}^{2+}$  ( $k$ ). An index is 1 (0) if the binding site is occupied (unoccupied). The conducting state 110 is highlighted in green. Panel (b) shows the transition rates on the front and back of the die. Panel (c) shows the transitions between the front and back faces. Binding rates are denoted  $\alpha$  and depend linearly on the corresponding concentration ( $\alpha_i = \hat{\alpha}_i[\text{IP}_3]$  for  $i = 1, 3$  and  $\alpha_i = \hat{\alpha}_i[\text{Ca}^{2+}]_i$  for  $i = 2, 4, 5$ ), while unbinding rates are denoted  $\beta$  and are constants. Parameters are according to Table I.

mation about extracellular stimuli (calcium signaling) [37,38]. The characteristic short periodic increases in the intracellular  $\text{Ca}^{2+}$  concentration that carry the information can be caused either by an influx of  $\text{Ca}^{2+}$  from the extracellular medium or by a release of  $\text{Ca}^{2+}$  from an intracellular store, the endoplasmic reticulum (ER). In both cases, stochastic transitions between discrete states of the ion channels give rise to macroscopic fluctuations in the intracellular  $\text{Ca}^{2+}$  concentration. The De Young-Keizer model covers the case where the  $\text{Ca}^{2+}$  signal is evoked by the release of  $\text{Ca}^{2+}$  from the ER through the  $\text{IP}_3$  receptor channel. This receptor channel in turn is assumed to consist of three independent and identical subunits with three binding sites each: one for the second-messenger molecule  $\text{IP}_3$ , produced in the cell in response to an extracellular stimulus ( $\text{IP}_3$  pathway), and one activating  $\text{Ca}^{2+}$  binding site and one inhibiting  $\text{Ca}^{2+}$  binding site. The  $\text{Ca}^{2+}$  current through a single  $\text{IP}_3$  receptor channel is given by

$$I_{\text{Ca}} = c_1 x^{(1)}(t) x^{(2)}(t) x^{(3)}(t) ([\text{Ca}^{2+}]_{\text{er}} - [\text{Ca}^{2+}]_i), \quad (19)$$

where  $[\text{Ca}^{2+}]_{\text{er}}$  and  $[\text{Ca}^{2+}]_i$  are the ER and intracellular (cytosolic)  $\text{Ca}^{2+}$  concentrations,  $c_1$  is the volume ratio between the ER and the cytosol, and  $x^{(n)}(t)$  are dichotomous (two-valued) stochastic processes capturing the state of the three  $\text{IP}_3$  receptor subunits. The kinetics of a single subunit is described by the scheme shown in Fig. 3. The eight possible states shown in Fig. 3(a) result from the fact that each of the three binding sites can be in two possible states, occupied or unoccupied. The subunit states are labeled  $ijk$ , where  $i$ ,  $j$ , and  $k$  indicate whether the  $\text{IP}_3$ , activating  $\text{Ca}^{2+}$ , and inhibitory  $\text{Ca}^{2+}$  binding sites are occupied ( $i, j, k = 1$ ) or unoccupied ( $i, j, k = 0$ ). The entire channel is open when in all subunits the  $\text{IP}_3$  and activating  $\text{Ca}^{2+}$  binding sites are occupied and the inhibitory  $\text{Ca}^{2+}$  binding site is unoccupied, i.e., when all three subunits are in the 110 state, highlighted in green in Fig. 3(a). Put differently, every state is assigned a value according to  $x_{ijk} = \delta_{i1} \delta_{j1} \delta_{k0}$ , i.e., the value of the conducting state 110 is



1 and the value of every other state is 0. The transition rates between the states on the front and back faces of the cube are shown in Fig. 3(b), while the transition rates between the two faces are shown in Fig. 3(c). Binding rates are denoted  $\alpha$  and depend linearly on the  $\text{IP}_3$  or  $\text{Ca}^{2+}$  concentration according to the law of mass action ( $\alpha_i = \hat{\alpha}_i[\text{IP}_3]$  for  $i = 1, 3$  and  $\alpha_i = \hat{\alpha}_i[\text{Ca}^{2+}]_i$  for  $i = 2, 4, 5$ ), whereas unbinding rates are denoted  $\beta$  and are constants (we keep the original notation of De Young and Keizer in terms of  $\hat{\alpha}$  and  $\gamma = \beta/\hat{\alpha}$ , see Table I).

While De Young and Keizer considered the  $\text{IP}_3$  receptor and its subunits in the thermodynamic limit, we calculate the variance  $\sigma^2$ , correlation time  $\tau$  and noise intensity  $D$  for a single subunit  $x^{(n)}(t)$ . Note that these noise characteristics have no equivalent in the thermodynamic limit case. Although the noise intensity for the Markov chain can be calculated analytically, the expressions for the stationary probability vector  $\mathbf{p}$  and the auxiliary matrix  $F$  are lengthy. Therefore, we determine these two statistics numerically by inverting the transition rate matrix  $W$ . Since  $W$  does not have full rank, this requires some manipulation, that we mentioned already in Sec. II and are more detailed below.

To compute the stationary probability vector  $\mathbf{p}$ , we implement the normalization condition by replacing all entries in an arbitrary row of  $W$  with ones, and the corresponding entry in the zero vector on the l.h.s. of the stationary master equation [Eq. (6)] with a one. This removes a redundant row in  $W$ , which can be obtained by linear combination of the other rows, and replaces it with the normalization condition  $\sum_i p_i = 1$ . The same trick is used to compute the auxiliary matrix  $F$ , again replacing all entries in a row of  $W$  with ones and the corresponding row of the matrix  $P_0 - \mathbb{1}$  on the l.h.s. of Eq. (13) with zeros. This satisfies the conditions  $\sum_i f_{ij} = 0$ .

The results for three statistics are shown in Fig. 4. In all cases, the numerically calculated values show excellent agreement with the theoretical predictions, demonstrating that the method is applicable even when the transition rate matrix is more complicated. Furthermore, the results show that the variance alone is an insufficient measure to quantify the effect of a random process on a driven variable. For example, while the variance is nearly constant for low values of  $[\text{Ca}^{2+}]_i$ , the noise intensity shows a pronounced maximum for an intermediate value.

## V. VOLTAGE-GATED CHANNELS: MODELS OF STOCHASTIC $\text{K}^+$ AND $\text{Na}^+$ CHANNELS

As a third and final example, we calculate the noise intensity for two Markov chains, as used in stochastic variants of the Hodgkin-Huxley model to describe the gating of the potassium ( $\text{K}^+$ ) and sodium ( $\text{Na}^+$ ) channels [39–41]. Similar to the example discussed in the previous section, microscopic transitions between different discrete states of the ion channels lead to stochastic ion currents and eventually to macroscopic fluctuations, here in the voltage of an excitable membrane. We emphasize that we now consider the characteristics of the current through an entire ion channel ( $\text{K}^+$  or  $\text{Na}^+$ ), in contrast to the subunit activity addressed in the previous section.

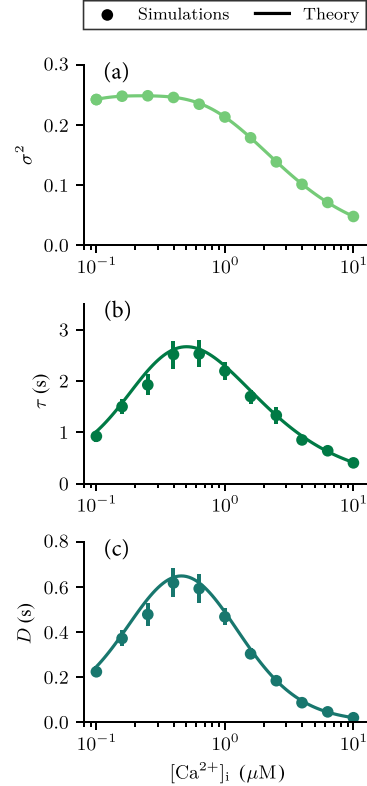


FIG. 4. Statistical measures of a stochastic  $\text{Ca}^{2+}$  channel subunit. Panels (a)–(c) show the variance  $\sigma^2$ , correlation time  $\tau$ , and noise intensity  $D$  as a function of the intracellular calcium concentration  $[\text{Ca}^{2+}]_i$  for a stochastic  $\text{IP}_3$  receptor subunit governed by the scheme illustrated in Fig. 3. Vertical lines indicate the standard error calculated from ten simulations. The variance and noise intensity are calculated according to Eq. (7) and Eq. (12), respectively. The correlation time is determined as the ratio  $\tau = D/\sigma^2$ . Parameters are according to Table I and  $\Delta t = 10^{-4}$  s,  $T = 100$  s.

The classical Hodgkin-Huxley model describes the dynamics of the membrane potential  $V$  and the generation of an action potential in a neuron by means of a passive leak current, a voltage-dependent  $\text{K}^+$  current, and a voltage-dependent  $\text{Na}^+$  current [42,43]. In a stochastic formulation the latter two currents can be expressed by

$$\begin{aligned} I_{\text{K}} &= g_{\text{K}} n^{(1)}(t) n^{(2)}(t) n^{(3)}(t) n^{(4)}(t) (V - E_{\text{K}}), \\ I_{\text{Na}} &= g_{\text{Na}} m^{(1)}(t) m^{(2)}(t) m^{(3)}(t) h^{(1)}(t) (V - E_{\text{Na}}), \end{aligned} \quad (20)$$

where  $g_{\text{K}}$  and  $g_{\text{Na}}$  are the maximal conductances and  $E_{\text{K}}$  and  $E_{\text{Na}}$  are the reversal potentials. In our case, the variables  $n^{(i)}$ ,  $m^{(j)}$ , and  $h^{(k)}$  are Markovian dichotomous processes that capture the state of the subunits in a single  $\text{K}^+$  or  $\text{Na}^+$  channel [44]. In accordance with Eq. (20), the  $\text{K}^+$  channel consists of four activation gates of type  $n$ , whereas the  $\text{Na}^+$  channel consists of three activation gates of type  $m$  and one inactivation gate of type  $h$ . Only when all subunits are open is the channel open.

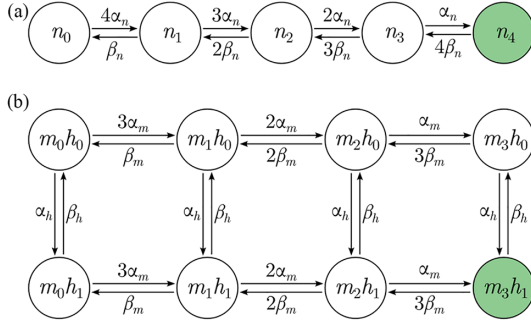


FIG. 5. State diagram of a  $K^+$  channel and a  $Na^+$  channel [41]. Panel (a) shows the five-state model of a stochastic  $K^+$  channel. The five states represent the number of activated  $n$ -type subunits (0 to 4) of the  $K^+$  channel. The transition rates are given above/below the arrows. All four subunits must be activated ( $n_4$ ) for the  $K^+$  channel to open. Panel (b) shows the eight-state model of a stochastic  $Na^+$  channel. The eight states represent the number of activated  $m$ -type (0 to 3) and deactivated  $h$ -type (0 to 1) subunits of the  $Na^+$  channel. All three subunits of type  $m$  must be activated and the subunit of type  $h$  must be deactivated ( $m_3h_1$ ) for the  $Na^+$  channel to open.

In the original Hodgkin-Huxley model, the gating variables are deterministic quantities bounded between zero and one and governed by the differential equation

$$\tau_z(V)\dot{z} = \alpha_z(V)(1 - z) - \beta_z(V)z, \quad (21)$$

with  $z = n, m, h$ . In this case,  $n, m$ , and  $h$  represent the fraction of open subunits in a large ensemble. However, Eq. (21) can also be interpreted as  $z(t)$  describing the probability of a single subunit taking a certain state in a two-state system with voltage-dependent transition rates  $\alpha_z(V)$  and  $\beta_z(V)$  (similar to Fig. 1). This insight allows to formulate stochastic variants of the Hodgkin-Huxley model consistent with the deterministic model in the thermodynamic limit, where the state of each subunit is represented by a Markovian dichotomous noise with a mean governed by Eq. (21) [39,40]. In this formulation, the gating variables correspond to the fluctuating fraction of open subunits in a finite ensemble.

In the following we calculate the noise intensity of the ion current through a single  $K^+$  channel or a single  $Na^+$  channel. We already emphasized that the kinetics of a single subunit [ $n^{(i)}(t)$ ,  $m^{(j)}(t)$ , and  $h^{(k)}(t)$ ] can be described by a Markovian dichotomous noise with a transition rate matrix similar to the one used in Sec. III. One could be tempted to think that the noise intensity of the product of a number of independent random processes can be easily found from the intensities of the single factors. However, this is only true for certain special processes, such as those with an exponential correlation function. In general we are not aware of a simple relation between the intensities.

To calculate the noise intensity for the product, we need to formulate the transition rate matrix for the random processes  $x(t) = n^{(1)}(t)n^{(2)}(t)n^{(3)}(t)n^{(4)}(t)$  for the  $K^+$  channel or  $x(t) = m^{(1)}(t)m^{(2)}(t)m^{(3)}(t)h^{(1)}(t)$  for the  $Na^+$  channel. Here, we follow the formulation of [41] and use transition rate matrices corresponding to the state diagrams in Fig. 5, which provide alternative but still exact descriptions of the currents through the two ion channels. The five possible states for the

TABLE II. Simulation parameters for  $K^+$  and  $Na^+$  channels in the Hodgkin-Huxley model [45].

Parameter	Value
$\alpha_n$ (ms <sup>-1</sup> )	$0.01(V + 55)/\{1 - \exp[-0.1(V + 55)]\}$
$\alpha_m$ (ms <sup>-1</sup> )	$0.1(V + 40)/\{1 - \exp[-0.1(V + 40)]\}$
$\alpha_h$ (ms <sup>-1</sup> )	$0.07 \exp[-0.05(V + 65)]$
$\beta_n$ (ms <sup>-1</sup> )	$0.125 \exp[-0.0125(V + 65)]$
$\beta_m$ (ms <sup>-1</sup> )	$4 \exp[-0.0556(V + 65)]$
$\beta_h$ (ms <sup>-1</sup> )	$1/\{1 + \exp[-0.1(V + 35)]\}$
$g_K$ (mS)	36
$g_{Na}$ (mS)	120
$E_K$ (mV)	-77
$E_{Na}$ (mV)	50

$K^+$  channel [Fig. 5(a)] result from the fact that the subunits are identical and independent. Therefore, it is sufficient to describe the number of subunits in the activated state. In this formulation, the transition rate from the state  $n_3$  (three activated  $n$ -type subunits) to  $n_4$  is  $\alpha_n$ , the rate at which the last deactivated gate is activated, and the transition from  $n_3$  to  $n_2$  is  $3\beta_n$ , the rate at which one out of three activated gates deactivates (see Refs. [41,45]). The entire  $K^+$  channel is considered open when all gates are activated, i.e., the value of the state  $n_4$  is 1 and the value of every other state is 0. Similarly, a reduced state diagram can be formulated for the  $Na^+$  channel [Fig. 5(b)]. In this case, the number of activated  $m$ -type subunits and number of inactivated  $h$ -type subunit must be distinguished, resulting in eight different states. The  $K^+$  channel is considered open, when all three  $m$ -type subunits are activated and the  $h$ -type subunits deactivated, i.e., the value of the state  $m_3h_1$  is 1 and the value of every other state is 0.

In Fig. 6 we compare simulation results and theoretical predictions of the open probability, variance, correlation time, and noise intensity of the stochastic  $K^+$  and  $Na^+$  currents according to Eq. (20) where the product of the gating variables,  $x(t) = n^{(1)}(t)n^{(2)}(t)n^{(3)}(t)n^{(4)}(t)$  in case of the  $K^+$  channel and  $x(t) = m^{(1)}(t)m^{(2)}(t)m^{(3)}(t)h^{(1)}(t)$  in case of the  $Na^+$  channel are described by a single random process, governed by the Markov schemes illustrated in Figs. 5(a) and 5(b), respectively. In both cases, the numerical computations agree with the theoretical predictions, demonstrating that the method is applicable to the stochastic Hodgkin-Huxley model. However, we note that our method relies on the assumption of a clamped voltage.

Regarding the interpretation of the obtained curves, we first note that the two upper panels agree with the deterministic open probability of the classical Hodgkin-Huxley model: A monotonically increasing function for the  $K^+$  channel [Fig. 6(a<sub>1</sub>)] and a nonmonotonic function for the  $Na^+$  channel [Fig. 6(b<sub>1</sub>)] due to the interplay between activation and inactivation. The latter maximum implies maxima in the variance [Fig. 6(b<sub>2</sub>)] and the noise intensity [Fig. 6(b<sub>4</sub>)]. We note that there are also maxima in the characteristics of the  $K^+$  channel at different voltage values Figs. 6(a<sub>2</sub>)–6(a<sub>4</sub>). The maximum of the variance is plausible because the open prob-

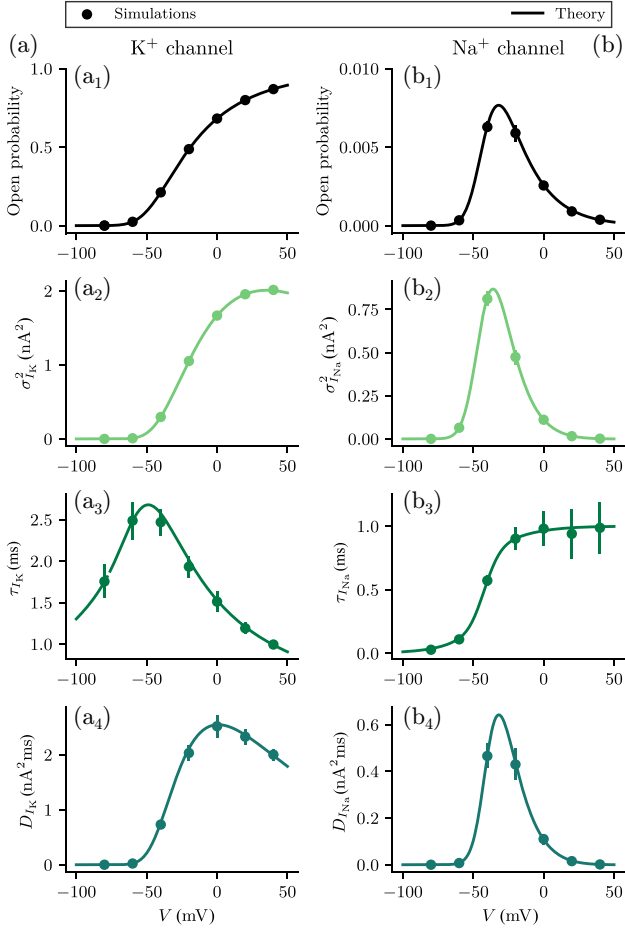


FIG. 6. Statistical measures of a stochastic  $K^+$  and  $Na^+$  channel. Panels (a), (b) show the open probability, variance  $\sigma^2$ , correlation time  $\tau$ , and noise intensity  $D$  as a function of the membrane potential  $V$  for the stochastic  $K^+$  and  $Na^+$  channels governed by the scheme illustrated in Figs. 5(a) and 5(b), respectively. Vertical lines indicate the standard error calculated from ten simulations. The variance and noise intensity are calculated according to Eq. (7) and Eq. (12), respectively. The correlation time is determined as the ratio  $\tau = D/\sigma^2$ . Parameters are according to Table II and  $\Delta t = 10^{-2}$  ms,  $T = 200$  ms.

ability reaches zero and one in the limit of extreme voltage values. This maximum then also entails a maximum of the noise intensity.

## VI. SUMMARY AND DISCUSSION

In this paper, we developed a general framework to characterize a noise process that is described by a finite Markov chain, i.e., by a Master equation with a finite number of states. More specifically, we demonstrated that the calculation of the noise intensity and correlation time of the process is only slightly more complicated than the computation of the steady state and its mean and variance, all in agreement with previous results from the literature [32–34]. We illustrated our general result by application to three cases: (i) the dichotomous noise (for which all characteristics are, of course, well known); (ii) a stochastic calcium channel subunit as it is used in the De Young-Keizer model; and (iii) sodium and potassium currents

as used in the Hodgkin-Huxley equation of action potential generation. In all these cases, our comparison to stochastic simulations of the underlying discrete dynamics agreed well with the analytical predictions of our formulas over a wide range of tested parameters.

The computation of noise intensity and correlation time has particular importance in the context of the so-called diffusion approximation. In several situations of interest the discrete fluctuations described by the Master equation can be well approximated by a white Gaussian noise. This stochastic process is fully characterized by its mean value and its noise intensity, for which we derived a simple expression above. Once this approximation has been made, the apparatus of nonlinear diffusion processes, in particular, the Fokker-Planck equation for the evolution of the probability density, can be used. To learn whether this approximation is really justified for a specific system, it is crucial to know the correlation time of the noise and to test whether it is much shorter than all other timescales in the system: only if this is the case are we permitted to neglect the temporal correlations of the noise process entirely. This may also apply in the more complicated situation in which both the mean and intensity depend on the dynamical variable(s) of the driven system, i.e., when there is a feedback between the dynamical variable(s) and the noise statistics. This is only one instance of a nonequilibrium situation, in which parameters of the system turn into time-dependent functions. It remains an interesting task for future investigations to examine how the calculations done in our paper can be generalized (at least approximately) in such cases.

Returning to the problem of the white-noise approximation, let us revisit the dynamics of the calcium subunit, for which the correlation time was shown in Fig. 4(b) as a function of the (clamped) calcium concentration. The maximum correlation time is below 3 seconds in this case. If we now take into account that calcium is *not* clamped but in fact obeys a dynamics on the timescale of tens of seconds to multiple minutes [46,47], we may justify to approximate the stochastic activity of the single subunit by a Gaussian white noise with a calcium-dependent mean value and a calcium-dependent noise intensity. This is true when the  $Ca^{2+}$  concentration is below some spiking threshold, and it does not include the dynamics that is responsible for the spike shape. For another calcium channel (cluster) model, this has been carried out in an integrate-and-fire type model of intracellular calcium excitability and thoroughly tested by us and a collaborator [30,31].

For the gating variables of the Hodgkin-Huxley model a similar argument may be possible. A naive version of the approximation is not justified to describe the generation of the action potential. It is exactly the nonlinear interplay between the voltage and gating dynamics that gives the action potential its characteristic shape, i.e., the upstroke of the spike caused by the positive feedback of sodium-channel opening upon an initial (and sufficiently strong) depolarization and the downstroke due to the slower inactivation of sodium channels and the opening of potassium channels. The membrane time constant in the original Hodgkin-Huxley model (roughly, the timescale of the voltage dynamics) is of the order of 3 ms [48] and thus comparable to the correlation time of the potassium

channel fluctuations [according to Fig. 6(b) around 2.5 ms for voltage values around the resting potential]. Hence, in this case it is recommendable to abstain from a white-noise approximation. Indeed, different approximation schemes that are based on having a large number of channels have been devised, see, e.g., the classical studies by Fox *et al.* [39,40] who approximated the gating dynamics by chemical Langevin equations, and more recent contributions which used stochastic shielding to obtain numerically efficient descriptions of the inherent stochasticity [6]. We note that our results are still useful because in the experiment the voltage *can and is routinely* clamped to a prescribed value and currents through specific channels can be isolated (methods for this are, for instance, discussed in the textbook by Izhikevich [42]), and in this situation our formulas give exact results for the characteristics of the respective current fluctuations. The same method can be applied to more complicated kinetic schemes of channel

states, see, e.g., the review on the many models of sodium channels [49].

Of course, the two above cases are more involved in the sense that the dynamics of the Markov chain itself are not always affected by the variable it drives. When the output of the Markov chain acts as an external noise on a system, no white-noise approximation has to be made and our results then simply provide the most important noise characteristics of this stochastic process, making it comparable to simpler noise models (white or low-pass filtered Gaussian noise, white Poissonian noise, or colored dichotomous noise).

## ACKNOWLEDGMENTS

L.R. and B.L. acknowledge the support provided by grant LI 1046/4-1 from the Deutsche Forschungsgemeinschaft.

- 
- [1] J. A. White, J. T. Rubinstein, and A. R. Kay, Channel noise in neurons, *Trends Neurosci.* **23**, 131 (2000).
- [2] A. D. Dorval, Jr. and J. A. White, Channel noise is essential for perithreshold oscillations in entorhinal stellate neurons, *J. Neurosci.* **25**, 10025 (2005).
- [3] T. Schwalger, K. Fisch, J. Benda, and B. Lindner, How noisy adaptation of neurons shapes interspike interval histograms and correlations, *PLoS Comp. Biol.* **6**, e1001026 (2010).
- [4] K. Fisch, T. Schwalger, B. Lindner, A. Herz, and J. Benda, Channel noise from both slow adaptation currents and fast currents is required to explain spike-response variability in a sensory neuron, *J. Neurosci.* **32**, 17332 (2012).
- [5] B. Moezzi, N. Iannella, and M. D. McDonnell, Ion channel noise can explain firing correlation in auditory nerves, *J. Comput. Neurosci.* **41**, 193 (2016).
- [6] S. Pu and P. J. Thomas, Resolving molecular contributions of ion channel noise to interspike interval variability through stochastic shielding, *Biol. Cybern.* **115**, 267 (2021).
- [7] N. Hohn and A. N. Burkitt, Shot noise in the leaky integrate-and-fire neuron, *Phys. Rev. E* **63**, 031902 (2001).
- [8] M. J. E. Richardson and W. Gerstner, Statistics of subthreshold neuronal voltage fluctuations due to conductance-based synaptic shot noise, *Chaos* **16**, 026106 (2006).
- [9] L. Wolff and B. Lindner, Mean, variance, and autocorrelation of subthreshold potential fluctuations driven by filtered conductance shot-noise, *Neural Comput.* **22**, 94 (2010).
- [10] M. J. E. Richardson and R. Swarbrick, Firing-rate response of a neuron receiving excitatory and inhibitory synaptic shot noise, *Phys. Rev. Lett.* **105**, 178102 (2010).
- [11] M. Brigham and A. Destexhe, Nonstationary filtered shot-noise processes and applications to neuronal membranes, *Phys. Rev. E* **91**, 062102 (2015).
- [12] F. Droste and B. Lindner, Exact analytical results for integrate-and-fire neurons driven by excitatory shot noise, *J. Comp. Neurosci.* **43**, 81 (2017).
- [13] H. Haken, H. Sauermann, C. Schmid, and H. D. Vollmer, Theory of laser noise in the phase locking region, *Z. Phys.* **206**, 369 (1967).
- [14] J. L. A. Dubbeldam, B. Krauskopf, and D. Lenstra, Excitability and coherence resonance in lasers with saturable absorber, *Phys. Rev. E* **60**, 6580 (1999).
- [15] W. S. Lam, P. N. Guzdar, and R. Roy, Effect of spontaneous emission noise and modulation on semiconductor lasers near threshold with optical feedback, *Int. J. Mod. Phys. B* **17**, 4123 (2003).
- [16] T. Schwalger, J. Tiana-Alsina, M. C. Torrent, J. Garcia-Ojalvo, and B. Lindner, Interspike-interval correlations induced by two-state switching in an excitable system, *Europhys. Lett.* **99**, 10004 (2012).
- [17] C. W. Gardiner, *Handbook of Stochastic Methods* (Springer, Berlin, 1985).
- [18] N. G. van Kampen, *Stochastic Processes in Physics and Chemistry* (North-Holland, Amsterdam, 1992).
- [19] D. T. Gillespie, The chemical Langevin equation, *J. Chem. Phys.* **113**, 297 (2000).
- [20] G. E. Uhlenbeck and L. S. Ornstein, On the theory of the Brownian motion, *Phys. Rev.* **36**, 823 (1930).
- [21] H. Risken, *The Fokker-Planck Equation* (Springer, Berlin, 1984).
- [22] P. Hänggi and P. Jung, Colored noise in dynamical-systems, *Adv. Chem. Phys.* **89**, 239 (1995).
- [23] W. Horsthemke and R. Lefever, *Noise-Induced Transitions: Theory and Applications in Physics, Chemistry, and Biology* (Springer, Berlin, 1983).
- [24] I. Bena, Dichotomous Markov noise: Exact results for out-of-equilibrium systems, *Int. J. Mod. Phys. B* **20**, 2825 (2006).
- [25] F. Droste and B. Lindner, Integrate-and-fire neurons driven by asymmetric dichotomous noise, *Biol. Cybern.* **108**, 825 (2014).
- [26] G. N. Farah and B. Lindner, Exponentially distributed noise - its correlation function and its effect on nonlinear dynamics, *J. Phys. A: Math. Theor.* **54**, 035003 (2021).
- [27] H. Risken, *The Fokker-Planck Equation*, 2nd edition (Springer, Berlin, 1989).
- [28] B. Lindner, The diffusion coefficient of nonlinear Brownian motion, *New J. Phys.* **9**, 136 (2007).
- [29] B. Lindner, Diffusion coefficient of a Brownian particle with a friction function given by a power law, *J. Stat. Phys.* **130**, 523 (2008).



- [30] L. Ramlow, M. Falcke, and B. Lindner, An integrate-and-fire approach to  $\text{Ca}^{2+}$  signaling. Part I: Renewal model, *Biophys. J.* **122**, 713 (2023).
- [31] L. Ramlow, M. Falcke, and B. Lindner, An integrate-and-fire approach to  $\text{Ca}^{2+}$  signaling. Part II: Cumulative refractoriness, *Biophys. J.* **122**, 4710 (2023).
- [32] M. Büttiker, Scattering theory of current and intensity noise correlations in conductors and wave guides, *Phys. Rev. B* **46**, 12485 (1992).
- [33] S. Hershfield, J. H. Davies, P. Hylgaard, C. J. Stanton, and J. W. Wilkins, Zero-frequency current noise for the double-tunnel-junction Coulomb blockade, *Phys. Rev. B* **47**, 1967 (1993).
- [34] C. Flindt, T. Novotný, and A. P. Jauho, Current noise in a vibrating quantum dot array, *Phys. Rev. B* **70**, 205334 (2004).
- [35] J. Hohnerkamp, *Stochastic Dynamical Systems: Concepts, Numerical Methods, Data Analysis* (Wiley/VCH, Weinheim, Germany, 1993).
- [36] G. W. De Young and J. Keizer, A single-pool inositol 1, 4, 5-trisphosphate-receptor-based model for agonist-stimulated oscillations in  $\text{Ca}^{2+}$  concentration, *Proc. Natl. Acad. Sci. USA* **89**, 9895 (1992).
- [37] M. J. Berridge, M. D. Bootman, and P. Lipp, Calcium - a life and death signal, *Nature (London)* **395**, 645 (1998).
- [38] D. E. Clapham, Calcium signaling, *Cell* **131**, 1047 (2007).
- [39] R. F. Fox and Y. N. Lu, Emergent collective behavior in large numbers of globally coupled independently stochastic ion channels, *Phys. Rev. E* **49**, 3421 (1994).
- [40] R. F. Fox, Stochastic versions of the Hodgkin-Huxley equations, *Biophys. J.* **72**, 2068 (1997).
- [41] C. Koch, *Biophysics of Computation - Information Processing in Single Neurons* (Oxford University Press, New York, 1999).
- [42] E. M. Izhikevich, *Dynamical Systems in Neuroscience: The Geometry of Excitability and Bursting* (MIT Press, Cambridge, MA, 2007).
- [43] W. Gerstner, W. M. Kistler, R. Naud, and L. Paninski, *Neuronal Dynamics From Single Neurons to Networks and Models of Cognition* (Cambridge University Press, Cambridge, England, 2014).
- [44] The state is described as activated or deactivated for  $n$  and  $m$ , and inactivated or deinactivated for  $h$  [45].
- [45] P. Dayan and L. F. Abbott, *Theoretical Neuroscience* (MIT Press, Cambridge, MA, 2001).
- [46] M. J. Boulware and J. S. Marchant, Timing in cellular  $\text{Ca}^{2+}$  signaling, *Curr. Biol.* **18**, R769 (2008).
- [47] K. Thurley, I. F. Smith, S. C. Tovey, C. W. Taylor, I. Parker, and M. Falcke, Timescales of  $\text{IP}_3$ -evoked  $\text{Ca}^{2+}$  spikes emerge from  $\text{Ca}^{2+}$  puffs only at the cellular level, *Biophys. J.* **101**, 2638 (2011).
- [48] A. L. Hodgkin and A. F. Huxley, A quantitative description of membrane current and its application to conduction and excitation in nerve, *J. Physiol.* **117**, 500 (1952).
- [49] J. Patlak, Molecular kinetics of voltage-dependent  $\text{Na}^+$  channels, *Physiol. Rev.* **71**, 1047 (1991).